

Supplementary Data:

Table S1: Clinical characteristics of nasopharyngeal carcinoma patients with high or low expression of lnc-MRPL39-2:1.

Table S2: The relationship between lnc-MRPL39-2:1 expression and survival analyzed by univariate and multivariable Cox regression analysis.

Table S3: miRNAs targeted to lnc-MRPL39-2:1 analyzed using the human lncRNA database LNCipedia (<https://lncipedia.org/>).

Fig. S1: Analysis of the differentially expressed lncRNAs and mRNAs between the NPC tumor tissues and para-tumor tissues. (A and B) Scatter plot of differentially expressed lncRNAs (A) and mRNAs (B) Between tumor and para-tumor tissues. Green lines represent fold change. (C and D) Volcano plots show differentially expressed lncRNAs (C) and Gene (D) in NPC and para-tumor tissues. Red plots represent significantly upregulated lncRNAs and mRNAs.

Fig. S2: Differentially expressed mRNAs were functionally classified via GO functional enrichment analysis and pathway annotation. The downregulated mRNAs were classified by biological processes (A) Cellular components (B)Molecular function (C) GO terms. The biological processes (D) Cellular components (E), and Molecular function (F) of the upregulated mRNAs in the NPC compared to para-tumor tissue groups. Pathway analyses of upregulated (G) and Downregulated mRNAs (H).

Fig. S3: Differentially expressed lncRNAs classified according to their distribution. (A) Dysregulated lncRNAs classified into intergenic, antisense overlapping, sense-overlapping, and bidirectional. (B) Differentially expressed lncRNAs distributed in various chromosomes. (C) Length distribution of the dysregulated lncRNAs.

Fig. S4: Differentially expressed lncRNAs in tissues and cells. (A, B) Expression of four upregulated (A) and three downregulated (B) lncRNAs measured by qPCR in five tumor and paired non-tumor tissues and NP69. *U6* was used as the loading control. The expression of lnc-MRPL39-2:1 was analyzed by RNA-FISH (C) and ISH assay (D).

Fig. S5: Full-length lnc-MRPL39-2:1 gene cloning. Gel electrophoresis (left panel) and sequencing (right panel) of nested PCR products from 3' RACE (A) and 5' RACE (B), respectively. Arrows indicate the purpose band. (C) Full-length human lnc-MRPL39-2:1 transcript.

Fig. S6: Lnc-MRPL39-2:1 promotes NPC cell growth and migration. (A and B) Lnc-MRPL39-2:1 suppression remarkably inhibits HONE1 cell metastasis. (A) Trans-well migration and

invasion assays were performed to determine the impact of lnc-MRPL39-2:1 on the migration and invasion of HONE1 cells. (B) Wound-healing assays in HONE1 cells transfected with shRNA-lnc-MRPL39-2:1 or empty vector, related to **Fig. 3D**. (C) Lnc-MRPL39-2:1 suppression significantly inhibits NPC cell colony formation, related to **Fig. 3H**. (D) Expression of lnc-MRPL39-2:1 as validated by qPCR. Effects of lnc-MRPL39-2:1 overexpression on proliferation (E) and colony-forming ability (F) were tested in CNE2 and HONE1 cells, related to **Fig. 3O** and **Fig. 3P**, respectively. (G) Apoptosis was analyzed using flow cytometry (statistics shown in **Fig. 3Q**) ($*P < 0.05$, $**P < 0.01$).

Fig. S7: HuR is responsible for lnc-MRPL39-2:1-mediated cell growth and migration. (A) HuR in cancer and para-cancer tissues was tested using IHC. (B) OS and PFS in patients with low or high HuR expression were analyzed. (C) The proliferation ability of NPC cells was verified using EDU assay, related to **Fig. 4G**. (D) The number of colonies of NPC cells was measured by the colony-formation assay, related to **Fig. 4H**. (E) Apoptotic NPC cells with lnc-MRPL39-2:1 or/and siHuR were tested using flow cytometry, related to **Fig. 4I**.

Fig. S8: β -Catenin pathway is involved with HuR in NPC tissue. (A) OS and PFS in the patients with a low or high expression of β -Catenin were analyzed. (B) Correlation between HuR and β -Catenin expression was measured in 30 NPC samples by qPCR. (C) The relationship between HuR and β -Catenin was validated using IHC in primary NPC tissue.

Fig. S9: The tumor samples were verified by the hematoxylin and eosin staining. The expression of Ki-67 and lnc-MRPL39-2:1 in the cancer tissue was tested by IHC and ISH, respectively.

Table S1

Characteristics	No. of patients n= 122	Expression of <i>Lnc-MRPL39-2</i>		P value
		Low, n (%)	High, n (%)	
Age				
≤40	46	11	35	1
>40	76	19	57	
Sex				
Male	87	23	64	0.497
Female	35	7	28	
T Stage				
T1-T2	43	17	26	0.008
T3-T4	79	13	64	
N Stage				
N0-N1	57	22	35	0.01
N2-N3	65	8	57	
M Stage				
M0	103	26	77	1
M1	19	4	15	
TNM Stage				
I-II	43	23	20	< 0.01
III-IV	79	7	72	
Local Failure				
Yes	27	8	19	0.613
No	95	22	73	
Regional Failure				
Yes	23	5	18	0.793
No	99	26	73	

A. All patients were restaged according to the 8th edition of the AJCC Cancer Staging Manual.
 Bold values indicate $P < 0.05$. P value is determined by χ^2 and Fisher's exact tests.

Table S2

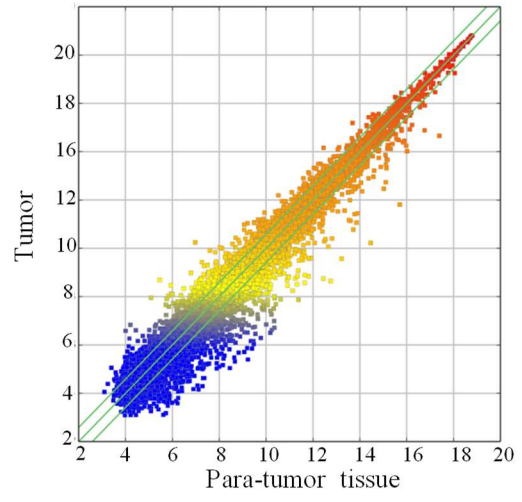
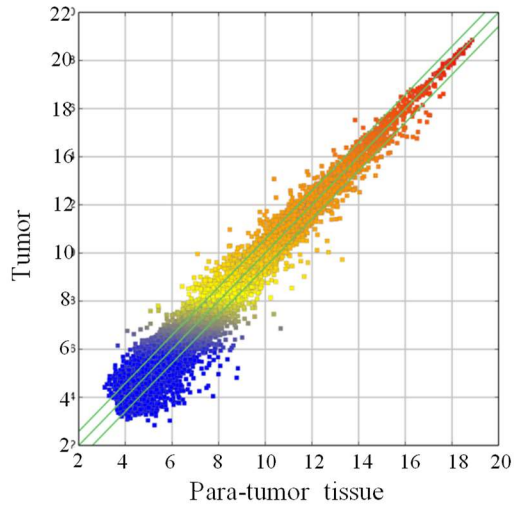
Parameters	Univariate analysis			Multivariate analysis		
	HR	95% CI	<i>P</i>	HR	95% CI	<i>P</i>
Overall survival						
Gender						
Male versus Female	1.32	0.95-2.45	0.41			
Age (years)						
≥40 vs. <40	1.23	0.85-1.62	0.36			
Histologic subtype						
DNKC vs. UDC	0.95	0.83-1.67	0.73			
TNM Stage						
III-IV vs. I-II	2.36	2.12-4.67	0.006	2.48	2.20-4.89	< 0.01
Lnc-MRPL39-2 expression						
High vs. Low	3.27	1.89-6.29	< 0.01	3.38	1.97-6.86	< 0.01
Progression Free Survival						
Gender						
Male versus Female	2.32	0.76-3.10	0.34			
Age (years)						
≥40 vs. <40	1.89	0.67-1.91	0.46			
Histologic subtype						
DNKC vs. UDC	1.06	0.76-1.93	0.67			
TNM stage						
III-IV vs. I-II	1.96	1.45-4.32	0.003	2.23	2.05-5.21	0.01
Lnc-MRPL39-2 expression						
High vs. Low	4.01	2.24-8.36	< 0.01	4.31	2.68-7.93	< 0.01

Table S3

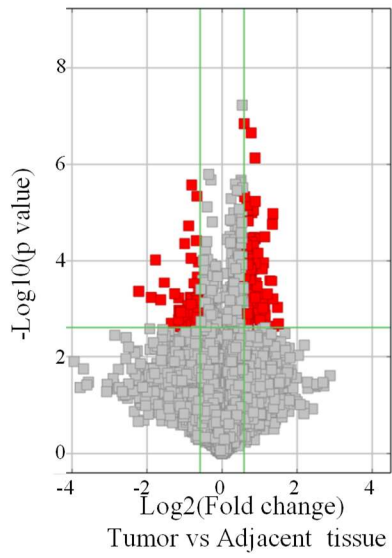
microRNA	MirTarget2 Score
has-miR-3613-3p	90.1
has-miR-3688-3p	89.75
has-miR-561-3p	89.57
has-miR-4775	88.72
has-miR-1283	86.78
has-miR-524-5p	86.38
has-miR-590-3p	83.21
has-miR-520d-5p	83.16
has-miR-144-5p	81.08
has-miR-4776-3p	77.88
has-miR-4668-3p	76.24
has-miR-548at-5p	76.07
has-miR-4769-3p	75.54
has-miR-934	74.13
has-miR-329	73.37
has-miR-362-3p	72.02
has-miR-16-1-3p	67.57
has-miR-551b-5p	67.4
has-miR-569	66.14
has-miR-3125	65.52
has-miR-875-5p	64.63
has-miR-187-5p	63.03
has-miR-4777-3p	60.64
has-miR-2053	60.36
has-miR-4763-3p	59.95
has-miR-501-5p	59.23
has-miR-4787-59	58.73
has-miR-3169	58.51
has-miR-518a-5p	57.17
has-miR-527	57.17
has-miR-4802-3p	56.77
has-miR-376c	56.25
has-miR-32-3p	55.7
has-miR-4690-5p	55.46
has-miR-1207-5p	54.15
has-miR-877-5p	53.84
has-miR-567	53.34
has-miR-592	52.37
has-miR-3916	52.35

Fig. S1

A



C



D

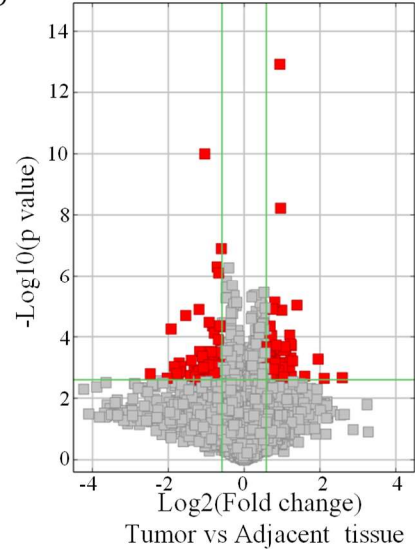


Fig. S2

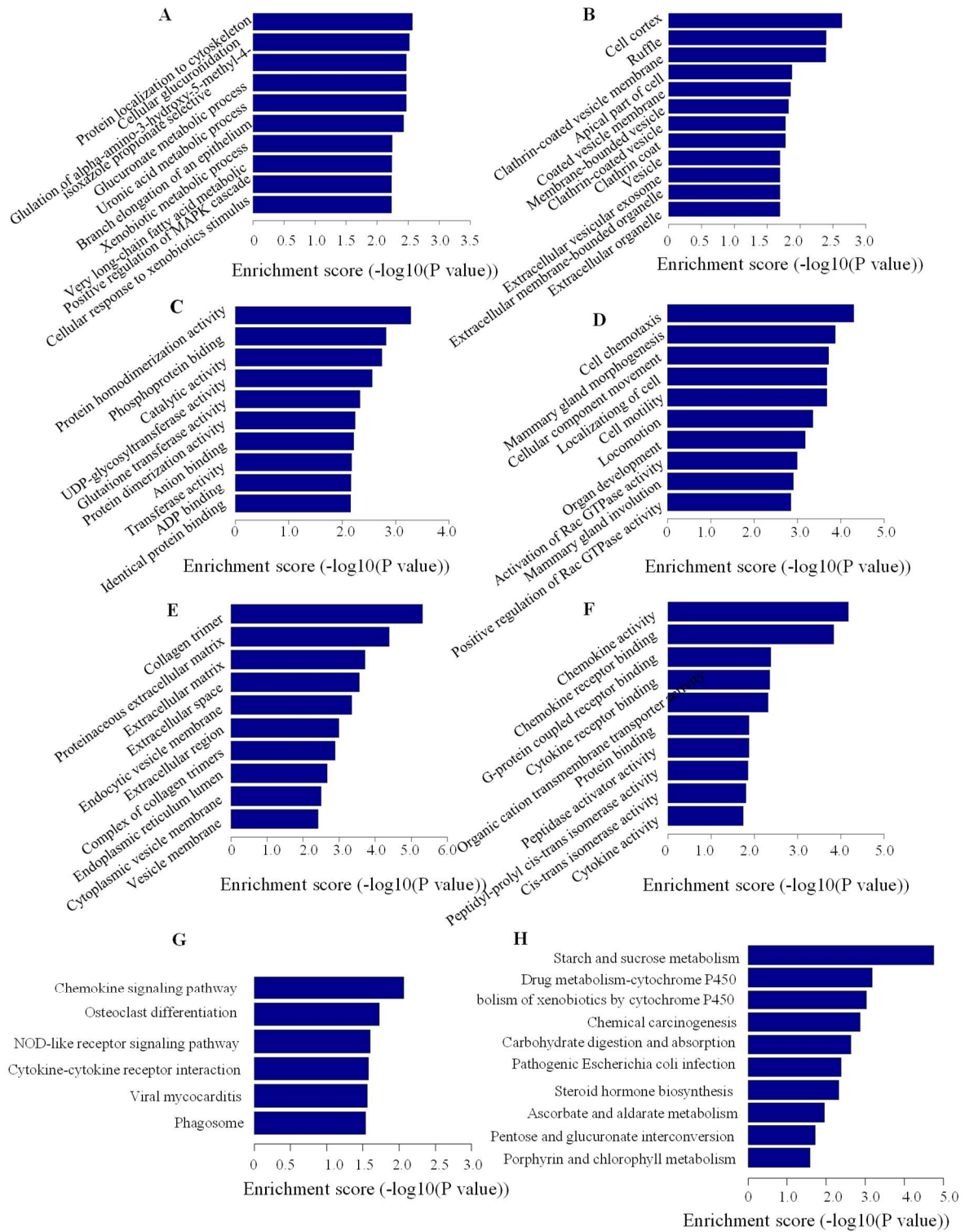


Fig. S3

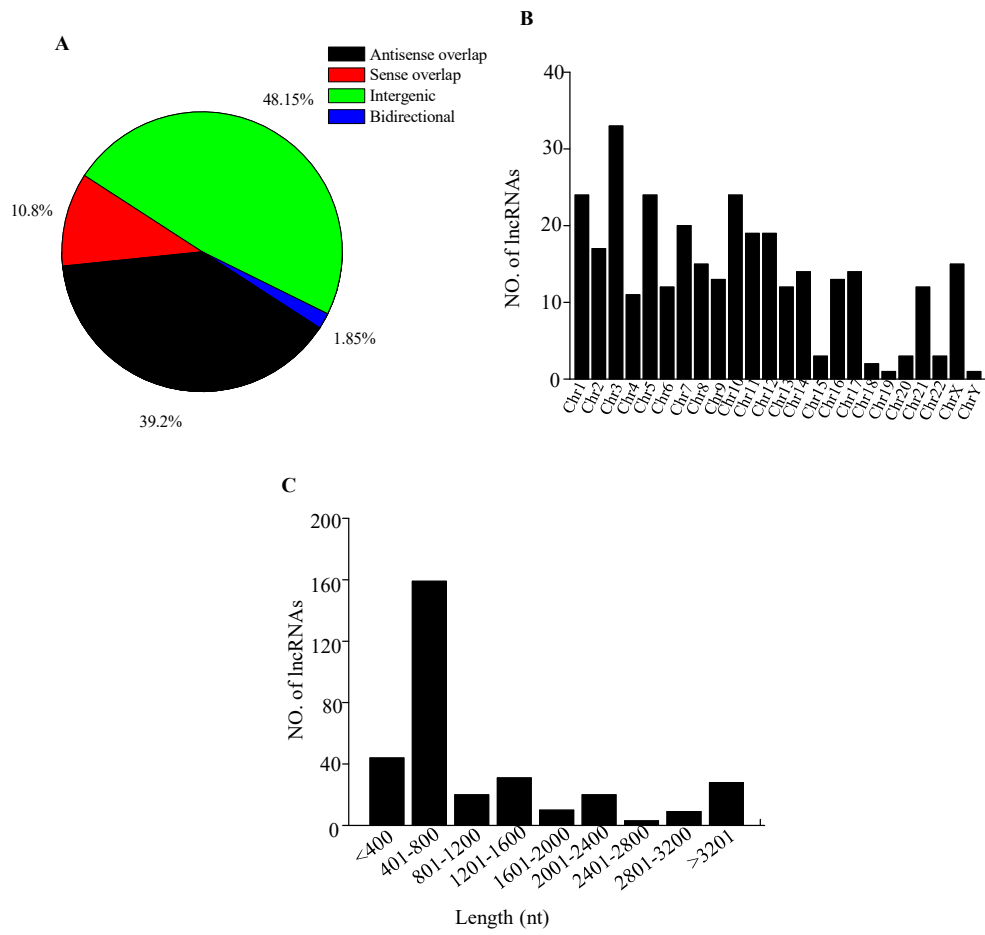


Fig. S4

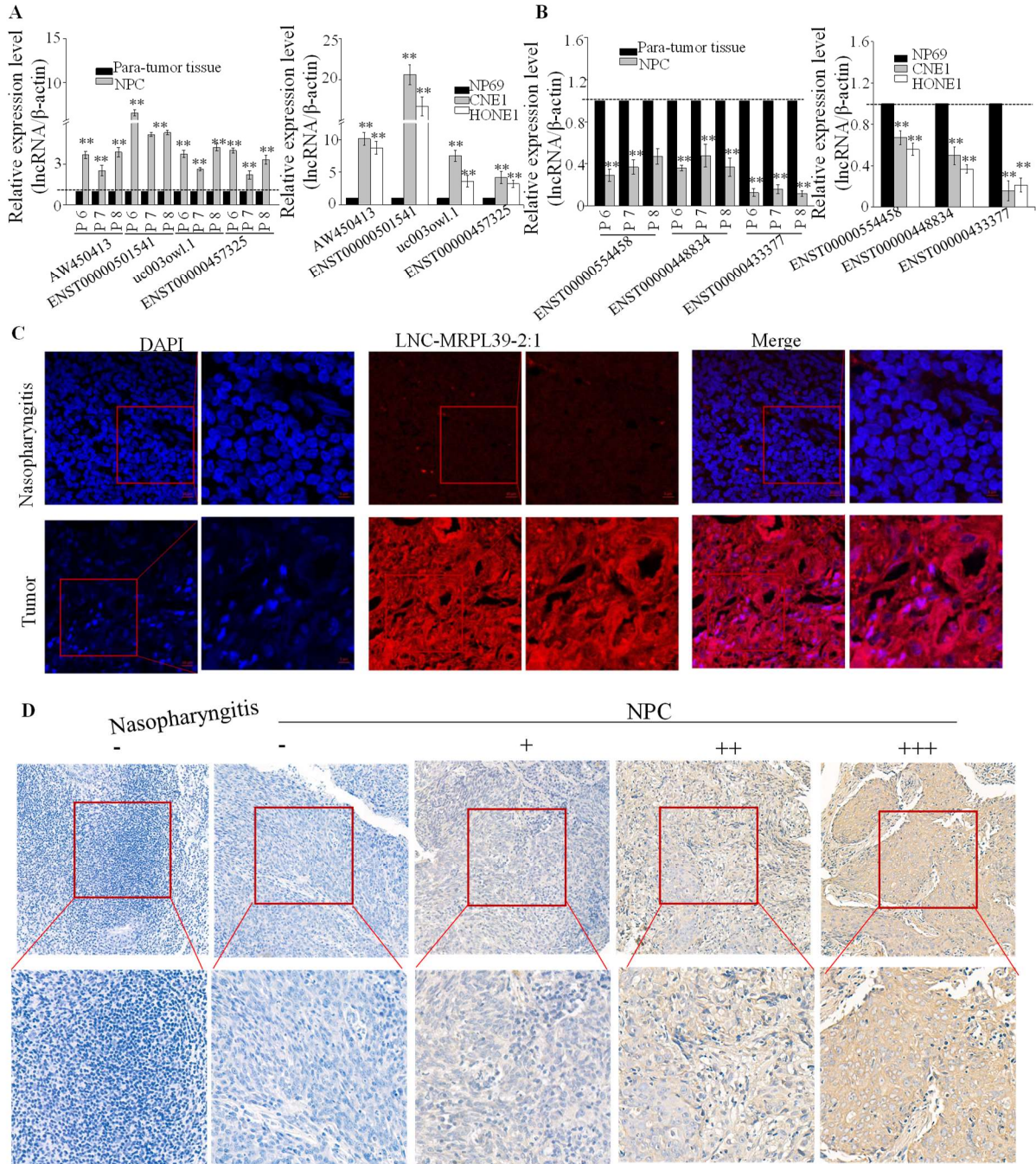


Fig. S5

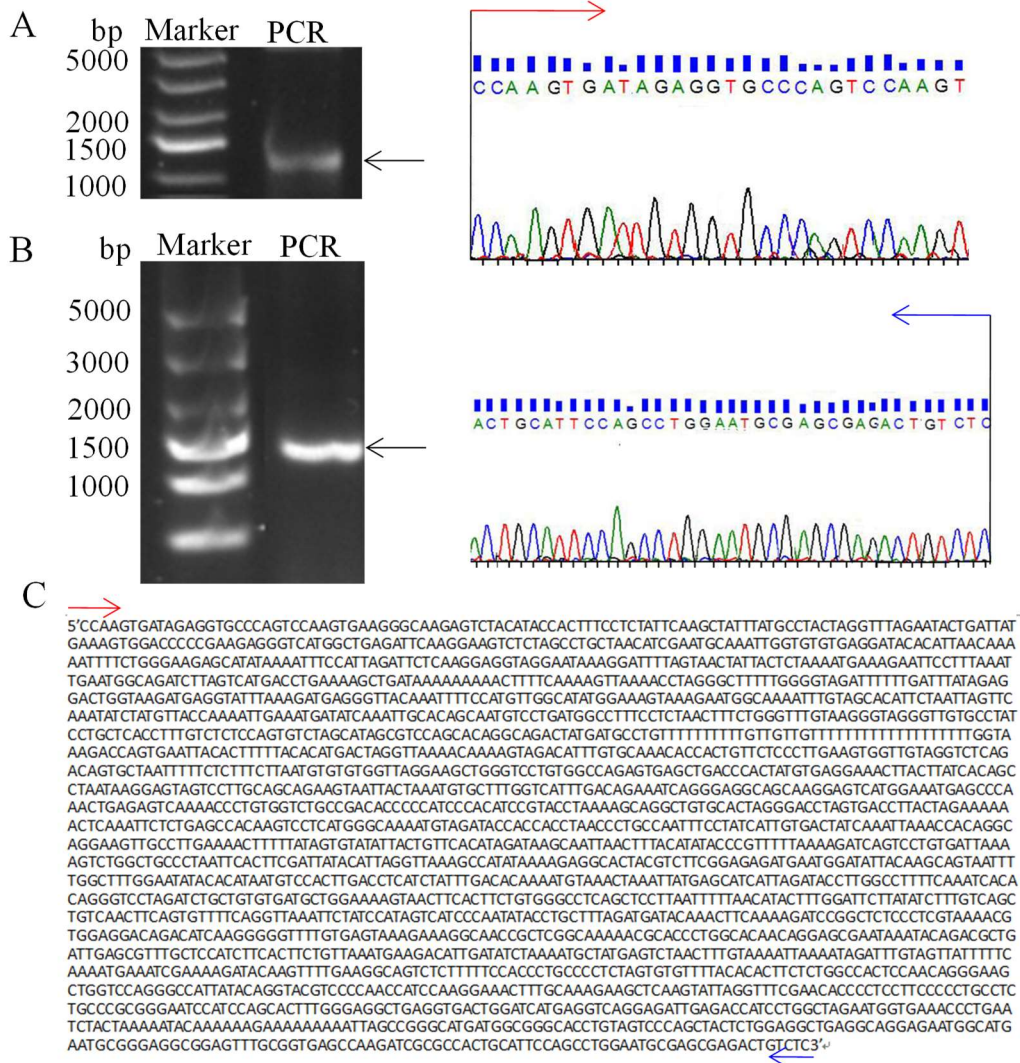


Fig. S6

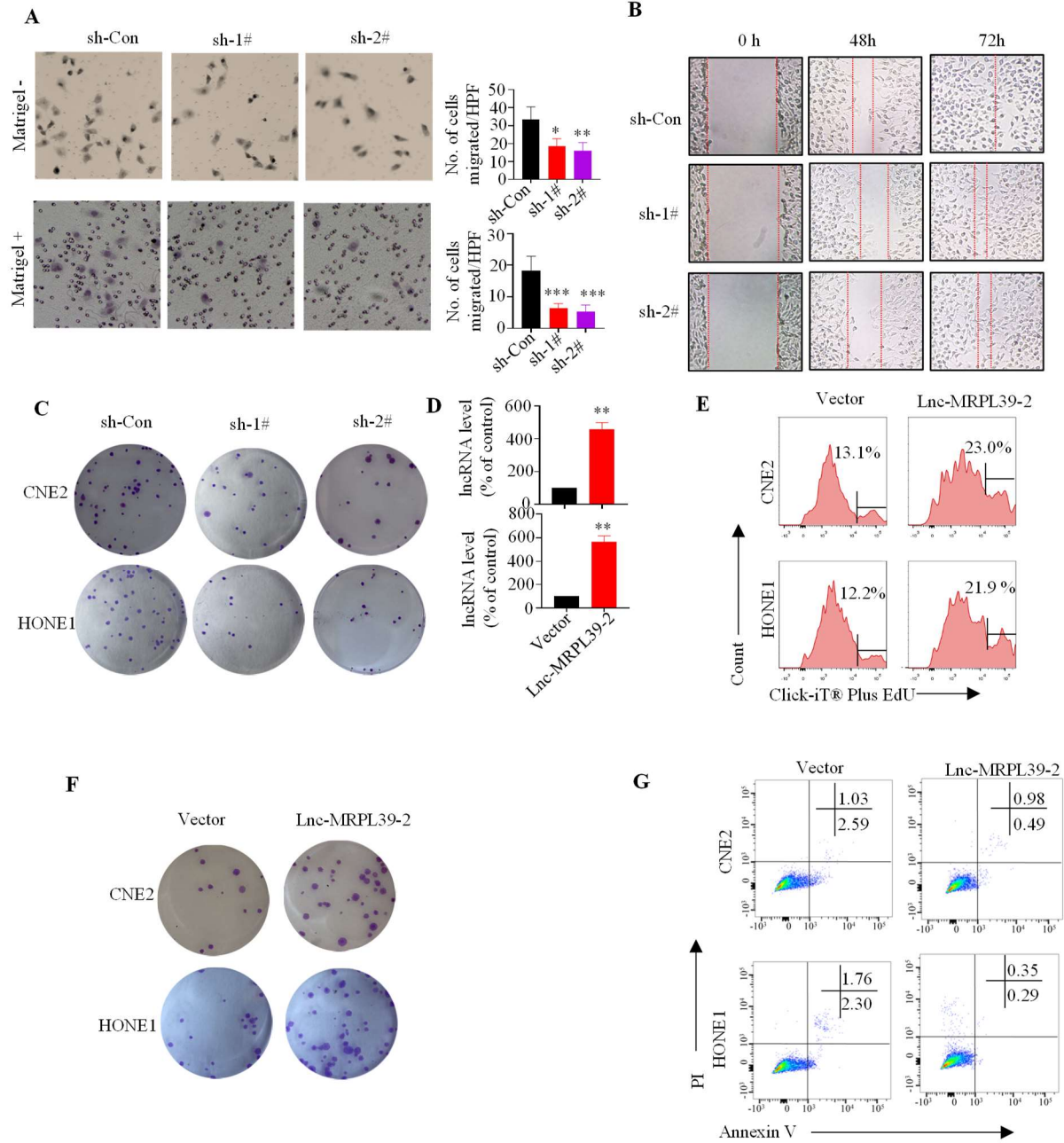


Fig. S7

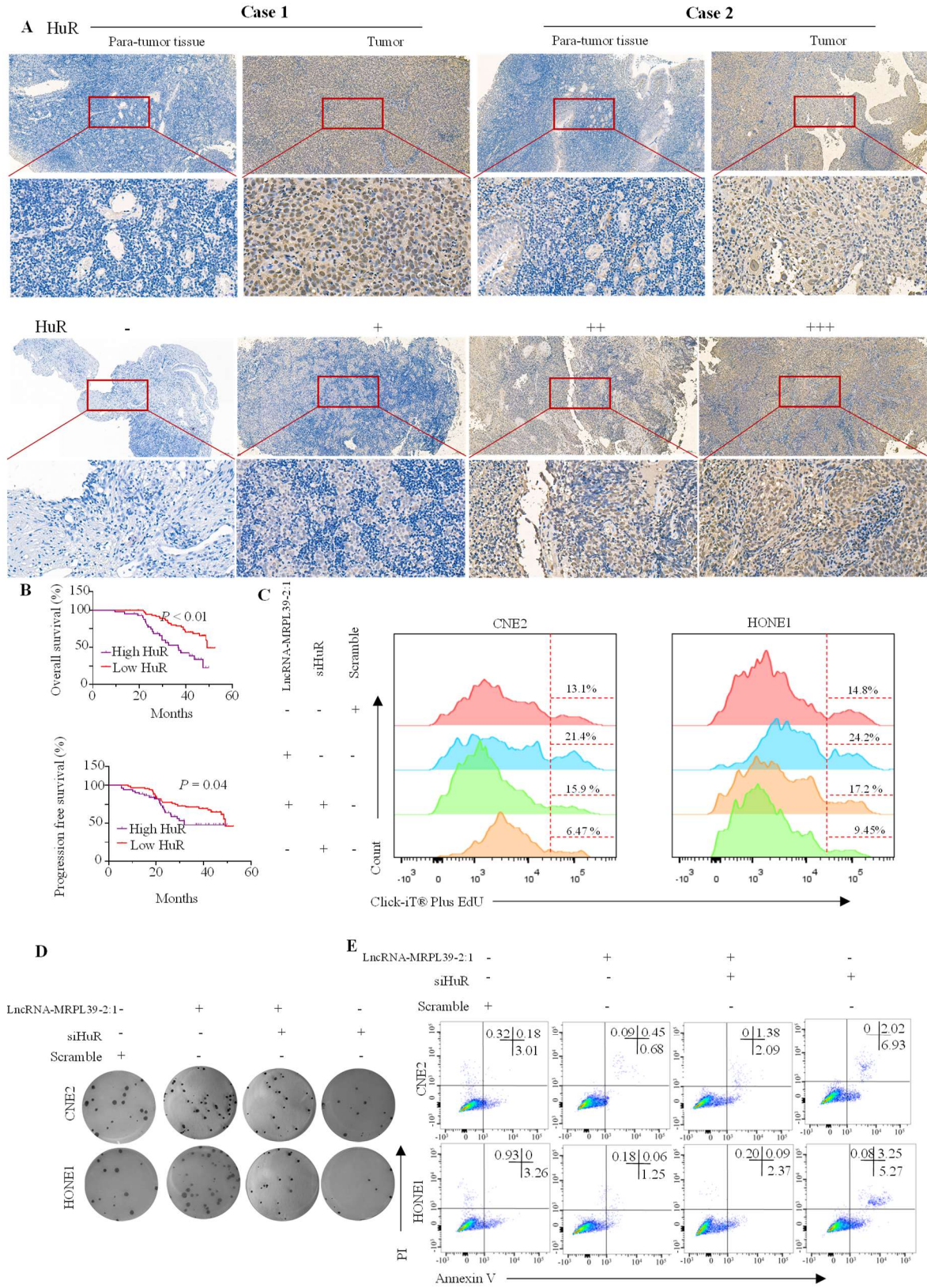


Fig. S8

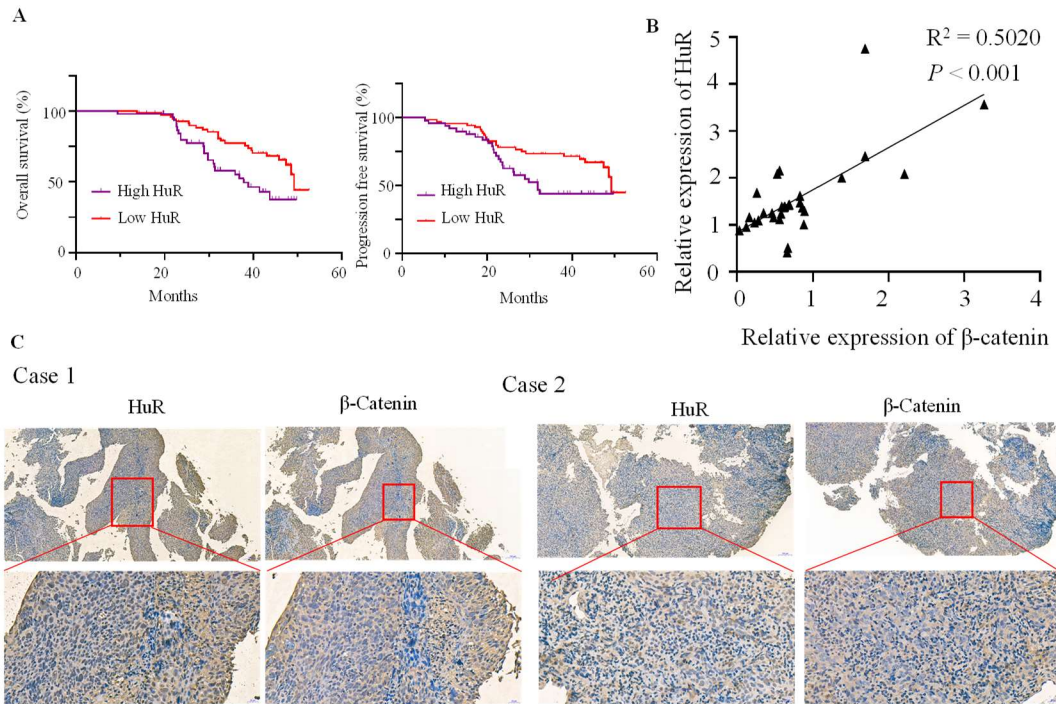


Fig. S9

